

PROCEEDINGS OF SPIE

SPIDigitalLibrary.org/conference-proceedings-of-spie

Electronic surface and heterostructure: band offsets in ternary wurtzite and zincblende III-nitrides

Tsai, Yi-Chia, Bayram, Can

Yi-Chia Tsai, Can Bayram, "Electronic surface and heterostructure: band offsets in ternary wurtzite and zincblende III-nitrides," Proc. SPIE 11686, Gallium Nitride Materials and Devices XVI, 116862C (5 March 2021); doi: 10.1117/12.2576374

SPIE.

Event: SPIE OPTO, 2021, Online Only

Electronic Surface and Heterostructure: Band Offsets in Ternary Wurtzite and Zincblende III-Nitrides

Yi-Chia Tsai and Can Bayram*

Department of Electrical and Computer Engineering, University of Illinois at Urbana–Champaign,
Urbana, IL 61801, USA

Holonyak Micro and Nanotechnology Laboratory, University of Illinois at Urbana–Champaign,
Urbana, IL 61801, USA

ABSTRACT

The band structures of wurtzite and zincblende III-nitrides are aligned by the electron affinities and the band gaps calculated using a unified hybrid density-functional theory. Based on the Anderson's electron-affinity rule, the conduction (and valence) band offsets of 1.60 (1.15), 2.47 (0.30), and 4.07 (1.45) eV have been extracted for wurtzite GaN/InN, AlN/GaN, and AlN/InN interfaces, where the conduction (and valence) band offsets of 1.85 (0.89), 1.32 (0.43), and 3.17 (1.32) eV have been procured for zincblende GaN/InN, AlN/GaN, and AlN/InN interfaces, respectively. The valence band edges of both wurtzite and zincblende ternary III-nitrides could be linearly interpolated because the dominant anion compositions at the valence band maximum have a weak dependence on the cation mole fractions. Contrarily, the large bowings on the conduction band edges are attributed to the cation-like nature. Both wurtzite and zincblende AlGaIn behaves differently from InGaIn and AlInN because (1) the conduction band edges at Γ -valley are composed of anion orbitals, which account for the linear relationship between the conduction band edges and the cation mole fractions, and (2) the conduction band edges of zincblende $\text{Al}_x\text{Ga}_{1-x}\text{N}$ shift from Γ - to X-valley when $x > 0.65$, which results in an anion-to-cation transition and leads to a large conduction-band-edge bowing.

Keywords: Zincblende GaN, Band Alignment, Density-Functional Theory, III-Nitrides, Zincblende, Quantum Wells

1. INTRODUCTION

The advent of modern solid-state lighting and wireless communications is attributed to the development of III-nitrides. For example, InGaIn with a band gap of 0.7–3.5 eV is commercially devised into blue light-emitting diodes (LEDs), white LEDs, and blue laser diodes that drive the demands for the next-generation micro/holo displays, optical data transmission, and visible light communications.¹ AlGaIn with a band gap of 3.5–6.3 eV has been devised into ultraviolet (UV) LEDs and high-electron-mobility transistors (HEMTs) that fulfill the urgent needs for rapid sterilization during COVID-19 pandemic and 5G wireless communications. Apart from the essential materials for active layers, more components are needed to maintain the efficiency and functionality of the devices. For the bipolar devices, large oscillation strength requires quantum well structures to improve the overlap between electron and hole spatial distributions. In contrast, for the ambipolar devices, the formation of two-dimensional electron gas for high-speed operations necessitates a heterostructure formed by adding a barrier layer, such as AlGaIn or AlN. These devices are made of wurtzite-phase (wz-) III-nitrides growing along the [0001] direction due to their stability and low defectivity. However, the inherent spontaneous and piezoelectric polarizations plague the radiative efficiency and the practicability for broad-spectrum applications. For instance, the internal quantum efficiency (IQE) of blue and red LEDs is fourfold of incumbent green-yellow LEDs. The engineering problem is known as the “Green Gap.” Likewise, the polarizations are the culprit that leads to normally-on conditions of HEMTs. A novel solution should feature the same benefits without suffering from the spontaneous and piezoelectric polarizations.

Fortunately, III-nitrides can also crystalize in a zincblende structure, which is naturally polarization-free along the $\langle 100 \rangle$ growth direction due to the centrosymmetry of the zincblende crystal structure. In addition to the polarization-free nature, zincblende III-nitrides also feature lighter electron and hole effective masses, higher radiative efficiencies,² higher hole mobilities (less carrier asymmetry),³ smaller p -type activation energies,⁴ higher optical gains,⁵ and less In incorporation needed for green–yellow emission.⁶ With all these benefits combined, the preliminary $k \cdot p$ simulations prevision the

* Corresponding author: Can Bayram (cbayram@illinois.edu)

improvements on laser diodes' optical gain and threshold current.⁷ Meanwhile, a record high band-to-band internal quantum efficiency of 29% in the UV spectrum has been achieved, which is more than twofold of 12% obtained from wurtzite III-nitrides.⁸ Devising zincblende III-nitrides photonics and electronics for a higher efficiency necessitates the use of quantum well geometry.

Given the mainstream research focus, the band alignments, including conduction and valence band offsets, have been primarily reported for wurtzite III-nitrides.^{9–11} The band alignments of zincblende III-nitrides remain either vague or unexplored. Specifically, a wide-range valence band offset of 0.25–1.00 eV was predicted for the zincblende AlN/GaN interface, while the band offsets of zincblende InN/GaN and AlN/InN are unclear. The large variation may be attributed to different approaches used to construct the band structures, such as hybrid density-functional theory, perturbation theory, and tight-binding model, and the energy reference, such as the vacuum level, average electrostatic potentials, charge neutrality levels, and branch-point energies.¹² It is paramount to use a unified approach for both wurtzite and zincblende III-nitrides to increase the simulation reliability. In this work, the natural band alignments of wurtzite and zincblende III-nitrides are calculated based on the Anderson's electron-affinity model, where the electric affinities are procured by hybrid density-functional theory.¹³

2. METHODOLOGY

The conduction and valence band edges of wurtzite and zincblende III-nitrides are aligned using Anderson's electron-affinity model. The electron affinities are calculated by band gaps and average electrostatic potentials obtained from hybrid density-functional theory implemented in the Vienna *ab initio* Simulation Package (VASP).¹⁴ Projected-augmented wave pseudopotentials delineate Al, Ga, In, and N's ionic potentials with a cut-off kinetic energy of 500 eV. In the following calculations, all the atoms and the crystal structures are fully relaxed to their equilibrium geometries where the interatomic forces and energy differences are smaller than $0.01 \text{ eV}\text{\AA}^{-1}$ and 10^{-6} eV , respectively. The band gaps and electron affinities are calculated separately in the bulk calculation and slab calculations, respectively. In the bulk calculations, a simple orthorhombic unit cell containing eight atoms with the lattice vector \vec{c} parallel to $(10\bar{1}0)$ is used to construct wurtzite III-nitrides, where a simple conventional cell containing eight atoms with the lattice vector \vec{c} parallel to (110) is used to build

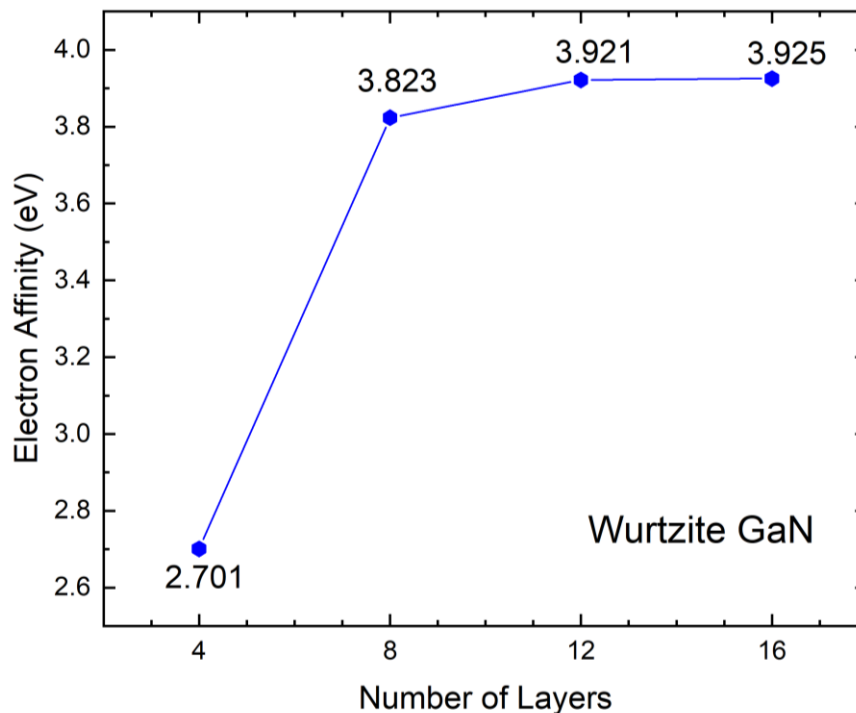


Fig. 1. The electron affinity of wurtzite GaN as a function of the number of atomic layers.

zincblende III-nitrides. The first Brillouin zones of the former and the latter geometries are sampled by $6 \times 4 \times 4$ and $5 \times 5 \times 5$ Monkhorst-Pack sets centered at the Γ point, respectively. Ground-state energies are commonly studied by local or semi-local functionals, such as local-density approximation (LDA) and generalized-gradient approximation (GGA). However, band gaps and electron affinities are related to the excited states, which are underestimated using LDA and GGA.^{15,16} Therefore, a hybrid functional–Heyd-Scuseria-Ernzerhof (HSE06)–is exploited to improve the accuracy of excited states by mixing Perdew-Becke-Ernzerhof (PBE), one type of GGA, exchange-correlation energy with Hartree-Fock exchange energy. The experimentally measured band gaps of wurtzite AlN, GaN, and InN are used to calibrate the mixing parameters. Table I tabulates the band gap of wurtzite and zincblende binary III-nitrides for $\alpha = 0.25, 0.30, 0.35$, and the optimal mixing parameter (α_{opt}). It shows that the band gaps vary linearly with respect to the increased α , therefore α_{opt} is determined by linear interpolation so that the calculated band gap is identical to the experimental band gap. The α_{opt} of wurtzite AlN, GaN, and InN are calibrated to be 0.341, 0.302, and 0.271, respectively. Likewise, the α_{opt} of ternary III-nitrides ($\text{Al}_x\text{Ga}_y\text{In}_{1-x-y}\text{N}$) are linearly interpolated using the α_{opt} of wurtzite AlN, GaN, and InN, formulated by

$$\alpha_{opt}(\text{Al}_x\text{Ga}_y\text{In}_{1-x-y}\text{N}) = 0.341 \cdot x + 0.302 \cdot y + 0.271 \cdot (1 - x - y),$$

where x and y are the Al and Ga mole fractions, respectively. It should be noted that the α_{opt} obtained using the measured band gaps of wurtzite III-nitrides are directly applied to zincblende III-nitrides. The purpose is to validate the method's accuracy while maintaining a unified approach that works for both wurtzite and zincblende III-nitrides. In the slab calculations, slabs of wurtzite and zincblende atomic structures are constructed to extract the vacuum energies relative to the average electrostatic potentials. By aligning the average electrostatic potentials obtained from the bulk calculations and the slab calculations, the energy difference between the vacuum energy and the conduction band minimum defined as electron affinity can be attained. The relationship is expressed by

$$\chi = (E_{vac} - \bar{V}_{slab}) - (E_g + VBM - \bar{V}_{bulk}),$$

where E_g , VBM , and \bar{V}_{bulk} are the band gap, the valence band maximum, and the average electrostatic potential energy obtained in the bulk calculations, while E_{vac} and \bar{V}_{slab} are the vacuum energy and the average electrostatic potential energy obtained from the slab calculations, respectively. To ensure the accuracy of vacuum energy, a fixed vacuum space of 18\AA is reserved for separating the slab from its periodic images in the $[10\bar{1}0]$ and $[110]$ directions for wurtzite and zincblende slabs, respectively. To ensure average electrostatic potential accuracy, both the wurtzite and zincblende slabs have a thickness of 12 atomic layers generated from the converged bulk structures. Fig. 1 shows the electron affinity of wurtzite GaN as a function of the atomic layers applied during the slab construction. The result shows that 12 atomic layers are thick enough to reproduce the bulk-like potential distribution at the center of slab.

3. RESULTS AND DISCUSSION

Figure 2(a) shows the conduction (E_c) and valence (E_v) band edges of wurtzite binary and ternary III-nitrides spanning from InN, GaN, AlN back to InN. The conduction band edges are linked by the black solid line, where the valence band edges are linked by the red dashed line. All the energies are shifted relative to the valence band edge of wurtzite GaN for convenience. Two distinct band edges evolve for each ternary wurtzite III-nitrides with 25% and 75% mole fractions. This

Table I. Band gap of wurtzite and zincblende binary III-nitrides calculated with different Hartree-Fock mixing parameters (a). The experimental band gaps are extracted from Ref. 18 unless stated otherwise.

Alloy	$E_g(\alpha = 0.25)$	$E_g(\alpha = 0.30)$	$E_g(\alpha = 0.35)$	α_{opt}	$E_g(\alpha = \alpha_{opt})$	E_g^{exp}
Wurtzite AlN	5.672	6.002	6.340	0.341	6.284	6.250
Wurtzite GaN	3.178	3.495	3.831	0.302	3.516	3.510
Wurtzite InN	0.680	0.922	1.167	0.271	0.773	0.780
Zincblende AlN	4.578	4.841	5.110	0.341	5.060	5.040 ¹⁹ , 5.340
Zincblende GaN	2.977	3.291	3.619	0.302	3.307	3.299
Zincblende InN	0.476	0.731	0.956	0.271	0.564	0.560 ²⁰

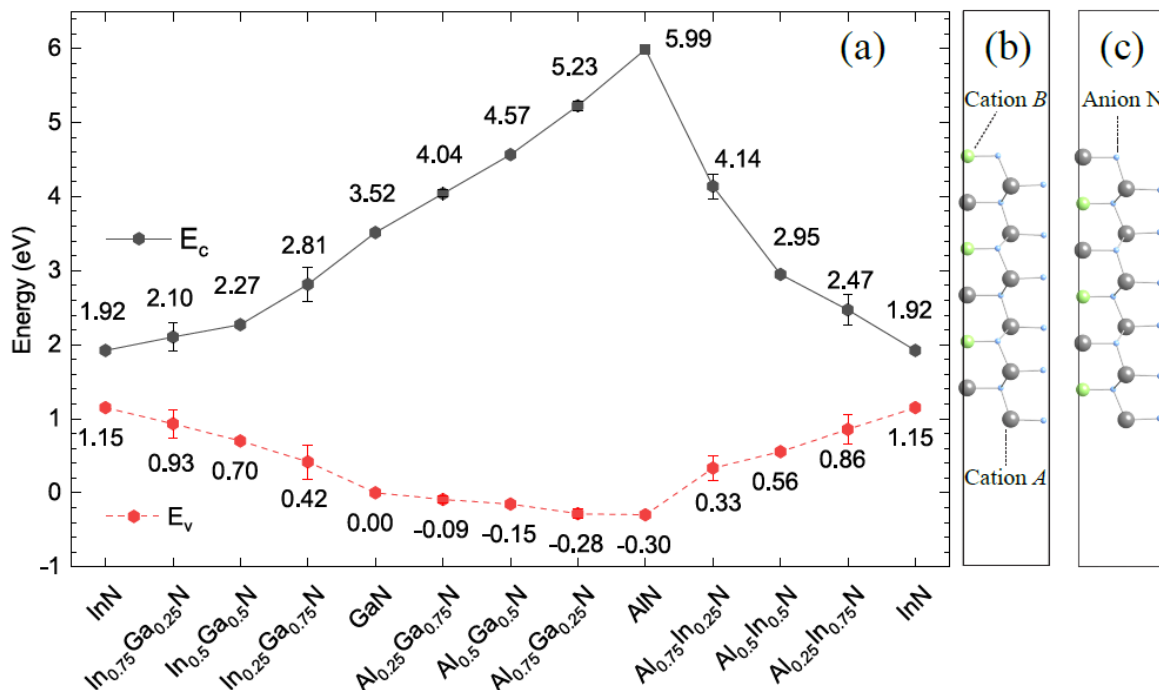


Fig. 2. (a) Conduction and valence band edges of binary and ternary wurtzite III-nitrides. The energies are shifted relative to the valence band maximum of wurtzite GaN. (b) and (c) illustrate the type-I and the type-II cation arrangements, respectively.

is because the electron affinity depends on the surface atomic arrangements, the surface stoichiometries, and the surface dipole moments. The crystal structure of wurtzite III-nitrides has two bases. Therefore, two different surface geometries can be built in the slab calculations, as illustrated in Fig. 2(b) and (c). One type of the surface geometries, defined as type-I cation arrangement shown in Fig. 2(b), has Al-N or In-N bonds parallel to the $(10\bar{1}0)$ plane and directly exposes to the vacuum space. The other surface geometry, defined as type-II cation arrangement shown in Fig. 2(c), has Al-N or In-N bonds parallel to the $(10\bar{1}0)$ plane, but the bonds do not directly expose to the vacuum space. When the cations are distributed uniformly, the two different surface stoichiometries result in identical and symmetric electron affinities, such as the wurtzite III-nitrides with 0%, 50%, and 100% mole fractions. In contrast, the surface stoichiometries are asymmetric between the type-I and the type-II cation arrangements for the wurtzite III-nitrides with 25% and 75% mole fractions. The variations in the electron affinities resulting from the surface stoichiometries are captured and found to have impacts on the conduction and valence band edges.

The wurtzite III-nitrides have type-I band alignments, where the band-edge differences in conduction and valence bands between arbitrary two alloys are the natural conduction and valence band offsets. In Fig. 2(a), the conduction (and valence) band offsets of wurtzite GaN/InN, AlN/GaN, and AlN/InN interfaces are 1.60 (1.15), 2.47 (0.30), and 4.07 (1.45) eV, leading to the ratios of conduction band offsets to band gap differences of 0.58, 0.89, and 0.74, respectively. The probed valence band offset of the wurtzite GaN/InN interface is 1.05 ± 0.25 eV,⁹ which is consistent with the calculation of 1.15 eV. For the wurtzite AlN/GaN interface, the calculated valence band offset of 0.30 eV agrees closely with the X-ray photoemission spectroscopy measurement of 0.3 ± 0.1 eV.¹⁰ Likewise, the reported valence band offset of wurtzite AlN/InN is 1.4 ± 0.1 eV,¹¹ which agrees with the simulation of 1.45 eV. The uncertainties in the experiments and the deviation between the experimental and the calculated values are attributed to (1) the overlook of defects, strains, and their impacts on surface polarity and (2) the chemical potency of reference core-levels assumed in the experiments.

By applying the same methodology, the conduction and valence band edges of zincblende III-nitrides are predicted and shown in Fig. 3, where the former is linked by the black line and the latter is linked by the red dashed line. The conduction and valence band edges are shifted relative to the valence band edge of zincblende GaN. It is worth noting that zincblende

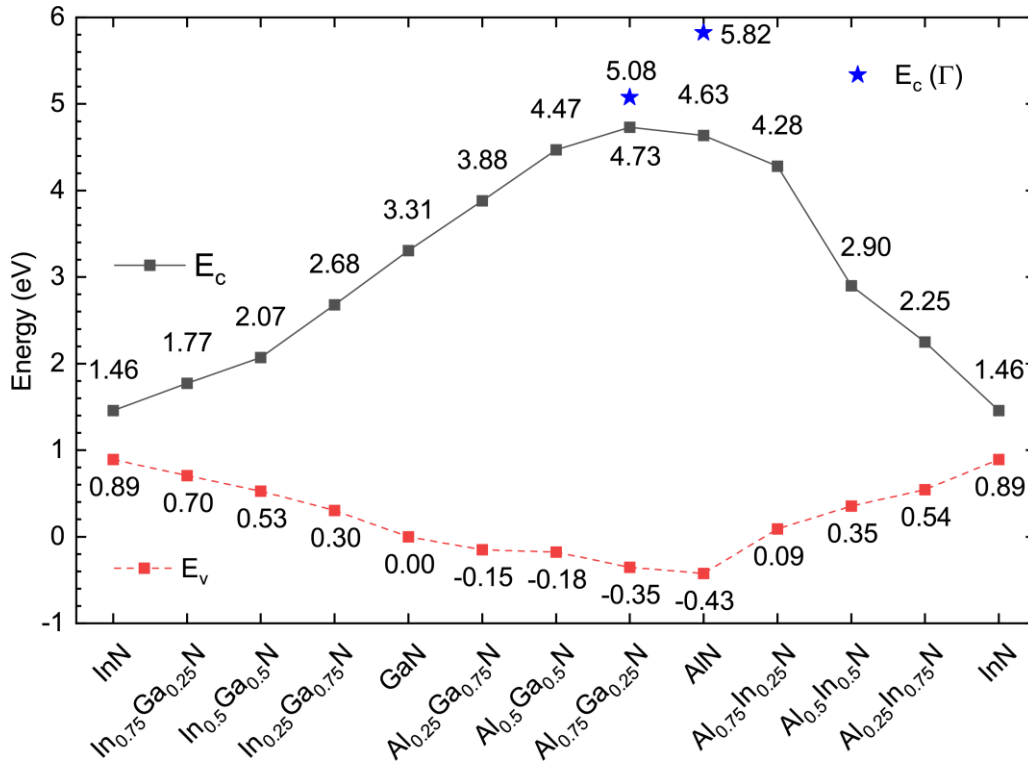


Fig. 3. Conduction and valence band edges of binary and ternary zincblende III-nitrides. The energies are shifted relative to the valence band maximum of zincblende GaN.

$\text{Al}_{0.75}\text{Ga}_{0.25}\text{N}$ and AlN are indirect-gap compounds, where the conduction band minima locate at X-valley. Using linear interpolation, the direct-to-indirect crossover point of zincblende $\text{Al}_{0.65}\text{Ga}_{0.35}\text{N}$ is identified when the conduction band minimum at Γ -valley has the same energy as that of X-valley. The crossover at 65% Al mole fraction is close to that of 70% Al mole fraction derived from the early calculation based on the LDA-1/2 approach.⁶ The blue-star symbols represent the conduction band edge at Γ -valley for zincblende $\text{Al}_{0.75}\text{Ga}_{0.25}\text{N}$ and AlN. The conduction and valence band offsets of zincblende GaN/InN, AlN/GaN, and AlN/InN interfaces are 1.85 (0.89), 1.32 (0.43), and 3.17 (1.32) eV, leading to the ratios of conduction band offsets to band gap differences of 0.68, 0.75, and 0.71, respectively. Given that the study of zincblende III-nitrides is still in a primitive stage, only the band offsets of the zincblende AlN/GaN interface have been measured experimentally. The conduction and valence band offsets of 1.4 ± 0.1 and 0.5 ± 0.1 eV are extracted from the intersubband transition energies of the zincblende AlN/GaN interface. The ratio between the conduction band offset and the band gap difference is 0.74 ± 0.05 .¹⁷ The conduction and valence band offsets of 1.22 and 0.42 eV had been predicted by fixing $\alpha = 0.25$ for both zincblende AlN and GaN.¹⁷ Although the valence band offset is close to the measurement because the valence band edge is a weak function of the mixing parameter, the conduction band offset significantly deviates from the measurement by more than 0.2 eV because the band gaps of AlN and GaN are underestimated. This evidences that the mixing parameters should be treated dynamically to procure accurate band gaps and conduction band offsets.

For the ternary III-nitrides, the valence band edges scale linearly with respect to the mole fractions of cations. By analyzing the element-projected electronic structures of wurtzite and zincblende binary III-nitrides, it is found that the valence band edges of III-nitrides are composed mainly of anion orbitals, which are less sensitive to the group-III alloying. Large bowings on the conduction band edges of wurtzite AlInN and InGaN are observed. These can be attributed to a cation-like character at the conduction band edges. However, the conduction band edge of wurtzite AlGaN scales linearly because the conduction band edge of wurtzite AlN at Γ -valley keeps an anion-like behavior. Given the similar orbital compositions, the conduction band edges of zincblende ternary III-nitrides evolve similarly with that of wurtzite counterparts, except for zincblende $\text{Al}_{0.75}\text{Ga}_{0.25}\text{N}$ and AlN. The conduction band minimum of zincblende AlGaN shifts from Γ -valley to X-valley when the Al mole fraction is larger than 0.65. When juxtaposed to the anion-like nature of Γ -valley, X-valley has a strong cation-like character. Such anion-to-cation transition accounts for the large bowing at the conduction band minima of

zincblende $\text{Al}_x\text{Ga}_{1-x}\text{N}$ with $x > 0.65$. The linear relationship is retained for the conduction band edges at the Γ -valley of zincblende AlGaN with arbitrary mole fractions.

4. CONCLUSION

In conclusion, the band diagrams of wurtzite and zincblende III-nitrides are aligned by the electron affinities and the band gaps procured from a unified hybrid density-functional theory. The natural conduction and valence band offsets are extracted from the band-edge differences. The conduction (and valence) band offsets of wurtzite GaN/InN, AlN/GaN, and AlN/InN interfaces are 1.60 (1.15), 2.47 (0.30), and 4.07 (1.45) eV, where the conduction (and valence) band offsets of zincblende GaN/InN, AlN/GaN, and AlN/InN interfaces are 1.85 (0.89), 1.32 (0.43), and 3.17 (1.32) eV, respectively. For the ternary III-nitrides in general, the linear dependence between the valence band edges and the cation mole fractions is attributed to the anion-like valence band maximum, while the large bowings of the conduction band edges are ascribed to the cation-like conduction band minimum. Special attention has been put on AlGaN since the conduction band edges of wurtzite and zincblende AlGaN at Γ -valley are mainly composed of anion orbitals, implying a linear dependence between the conduction band edges and the cation mole fractions. The large bowings of the conduction band edges of zincblende $\text{Al}_x\text{Ga}_{1-x}\text{N}$ with $x > 0.65$ are a result of anion-to-cation transition, where the conduction band minimum shifts from Γ -valley to X-valley.

This work is supported by the National Science Foundation Faculty Early Career Development (CAREER) Program under award number NSF-ECCS-16-52871. The authors acknowledge the computational resources allocated by the Extreme Science and Engineering Discovery Environment (XSEDE) with No. TG-DMR180075.

REFERENCES

- [1] DenBaars, S. P., Feezell, D., Kelchner, K., Pimputkar, S., Pan, C.-C., Yen, C.-C., Tanaka, S., Zhao, Y., Pfaff, N., Farrell, R., Iza, M., Keller, S., Mishra, U., Speck, J. S. and Nakamura, S., "Development of gallium-nitride-based light-emitting diodes (LEDs) and laser diodes for energy-efficient lighting and displays," *Acta Mater.* **61**(3), 945–951 (2013).
- [2] Lv, B., Tang, Y., Lou, S., Xu, Y. and Zhou, S., "Single p-n homojunction white light emitting diodes based on high-performance yellow luminescence of large-scale GaN microcubes," *J. Mater. Chem. C* **4**(23), 5416–5423 (2016).
- [3] Fernandez, J. R. L., Chitta, V. A., Abramof, E., Ferreira Da Suva, A., Leite, J. R., Tabata, A., As, D. J., Frey, T., Schikora, D. and Lischka, K., "Electrical properties of cubic InN and GaN epitaxial layers as a function of temperature," *Mater. Res. Soc. Symp. - Proc.* **595** (2000).
- [4] Tsai, Y.-C. and Bayram, C., "Mitigate Self-Compensation with High Crystal Symmetry: A First-Principles Study of Formation and Activation of Impurities in GaN," *Comput. Mater. Sci.* **190**(1), 110283 (2021).
- [5] Kim, C.-H. and Han, B.-H., "Valence subbands and optical gain in wurtzite and zinc-blende strained GaN/AlGaInN quantum wells," *Solid State Commun.* **106**(3), 127–132 (1998).
- [6] Tsai, Y.-C. and Bayram, C., "Structural and Electronic Properties of Hexagonal and Cubic Phase AlGaInN Alloys Investigated Using First Principles Calculations," *Sci. Rep.* **9**(1), 6583 (2019).
- [7] Machhadani, H., Tchernycheva, M., Sakr, S., Rigutti, L., Colombelli, R., Warde, E., Mietze, C., As, D. J. and Julien, F. H., "Intersubband absorption of cubic GaN/Al(Ga)N quantum wells in the near-infrared to terahertz spectral range," *Phys. Rev. B* **83**, 75313 (2011).
- [8] Liu, R., Schaller, R., Chen, C. Q. and Bayram, C., "High Internal Quantum Efficiency Ultraviolet Emission from Phase-Transition Cubic GaN Integrated on Nanopatterned Si(100)," *ACS Photonics* **5**(3), 955–963 (2018).
- [9] Martin, G., Botchkarev, A., Rockett, A. and Morkoç, H., "Valence-band discontinuities of wurtzite GaN, AlN, and InN heterojunctions measured by x-ray photoemission spectroscopy," *Appl. Phys. Lett.* **68**(18), 2541–2543 (1996).
- [10] Rizzi, A., Lantier, R., Monti, F., Lüth, H., Sala, F. Della, Carlo, A. Di and Lugli, P., "AlN and GaN epitaxial heterojunctions on 6H-SiC(0001): Valence band offsets and polarization fields," *Cit. J. Vac. Sci. Technol. B Microelectron. Nanom. Struct. Process.* **17**, 1674 (1999).
- [11] Kuo, C. T., Chang, K. K., Shiu, H. W., Liu, C. R., Chang, L. Y., Chen, C. H. and Gwo, S., "Natural band alignments

- of InN/GaN/AlN nanorod heterojunctions,” *Appl. Phys. Lett.* **99**(12), 122101 (2011).
- [12] Landmann, M., Rauls, E. and Schmidt, W. G., “Understanding band alignments in semiconductor heterostructures: Composition dependence and type-I-type-II transition of natural band offsets in nonpolar zinc-blende $\text{Al}_x\text{Ga}_{1-x}\text{N}/\text{Al}_y\text{Ga}_{1-y}\text{N}$ composites,” *Phys. Rev. B* **95**, 155310 (2017).
- [13] Tsai, Y.-C. and Bayram, C., “Band Alignments of Ternary Wurtzite and Zincblende III-Nitrides Investigated by Hybrid Density Functional Theory,” *ACS Omega* **5**(8), 3917–3923 (2020).
- [14] Kresse, G. and Hafner, J., “Ab initio molecular dynamics for liquid metals,” *Phys. Rev. B* **47**(1), 558–561 (1993).
- [15] Tran, F. and Blaha, P., “Accurate Band Gaps of Semiconductors and Insulators with a Semilocal Exchange-Correlation Potential,” *Phys. Rev. Lett.* **102**(22), 226401 (2009).
- [16] Mietze, C., Landmann, M., Rauls, E., Machhadani, H., Sakr, S., Tchernycheva, M., Julien, F. H., Schmidt, W. G., Lischka, K. and As, D. J., “Band offsets in cubic GaN/AlN superlattices,” *Phys. Rev. B - Condens. Matter Mater. Phys.* **83**(19), 1–10 (2011).
- [17] Mietze, C., Landmann, M., Rauls, E., Machhadani, H., Sakr, S., Tchernycheva, M., Julien, F. H., Schmidt, W. G., Lischka, K. and As, D. J., “Band offsets in cubic GaN/AlN superlattices,” *Phys. Rev. B* **83**, 195301 (2011).
- [18] Vurgaftman, I. and Meyer, J. R., “Band parameters for nitrogen-containing semiconductors,” *J. Appl. Phys.* **94**(6), 3675–3696 (2003).
- [19] Suzuki, T., Yaguchi, H., Okumura, H., Ishida, Y. and Yoshida, S., “Optical constants of cubic GaN, AlN, and AlGaIn alloys,” *Jpn. J. Appl. Phys.* **39**(Part 2, No. 6A), L497–L499 (2000).
- [20] Schörmann, J., As, D. J., Lischka, K., Schley, P., Goldhahn, R., Li, S. F., Löffler, W., Hetterich, M. and Kalt, H., “Molecular beam epitaxy of phase pure cubic InN,” *Appl. Phys. Lett.* **89**(26), 261903 (2006).